ISSN 0031-918X, Physics of Metals and Metallography, 2021, Vol. 122, No. 1, pp. 60–66. © Pleiades Publishing, Ltd., 2021.
Russian Text © The Author(s), 2021, published in Fizika Metallov i Metallovedenie, 2021, Vol. 122, No. 1, pp. 67–73.

## STRENGTH AND PLASTICITY

# Effect of Deformation Temperature on Formation of Ultrafine-Grained Structure in the Age-Hardenable Cu–Cr–Zr Alloy

**A. I. Morozova[a, b, *], A. N. Belyakov[a], and R. O. Kaibyshev[a]**

[a] *Belgorod State University, Belgorod, 308015 Russia*
[b] *National University of Science and Technology MISiS, Moscow, 119049 Russia*
**e-mail: morozova_ai@bsu.edu.ru*

Received March 27, 2020; revised August 18, 2020; accepted September 4, 2020

**Abstract**—The effect of the temperature of plastic deformation performed by equal channel angular pressing on the structure and physical and mechanical properties of the age-hardenable Cu–Cr–Zr alloy has been studied. Plastic deformation results in the formation of an ultrafine-grained structure in some regions with an average grain size smaller than 1 μm, a supersaturated solid solution decomposition, and the precipitation of disperse particles. The fraction of the supersaturated solid solution which is decomposed is shown to increase with increasing deformation temperature. The density of microshear bands, the dislocation density, and the fraction of high-angle boundaries and the ultrafine-grained structure increase with increasing volume fraction of disperse particles.

**Keywords:** Cu–Cr–Zr alloy, ECAP, microstructure, physical and mechanical properties, disperse particles
**DOI:** 10.1134/S0031918X21010087

## INTRODUCTION

Promising materials for the electrical industry are the heat-strengthened Cu–Cr–Zr alloys in which high electrical conductivity and strength can be achieved by forming an ultra-fine-grained (UFG) structure stabilized by disperse particles [1–3]. Such a microstructure can be formed by severe plastic deformation in combination with heat treatment (HT) [4]. The role of one of the main hardening components in Cu–Cr–Zr alloys is played by disperse particles. The Guinier–Preston zones, Cr, $Cu_5Zr$, $Cu_4Zr$, and $Cu_2CrZr$ particles precipitated in Cu–Cr–Zr alloys are mentioned in the literature [5–7]. Their chemical composition is difficult to determine precisely because of the small volume fraction (less than 1%) and the size of the second phase particles (2–4 nm). Disperse particles precipitated in Cu–Cr–Zr alloys have been established to improve the service properties of the alloys [8]. On the one hand, disperse particles provide precipitation hardening (100–150 MPa) [9], on the other hand, depletion of the supersaturated solid solution (SSS) of the copper matrix with alloying elements improves the conductive properties considerably [10]. Disperse particles are known to have a significant influence on the evolution of the microstructure and the physical and mechanical properties of alloys during deformation [11]. However, the majority of works devoted to the influence of severe plastic deformations were carried out on the Cu–Cr–Zr alloys after treatment aimed at obtaining a supersaturated solid solution, and the deformation was carried out at room temperature [1, 3, 4, 8]. Therefore, the effect of disperse particles formed during preliminary HT and deformation on the microstructure and properties of the alloys has not yet been investigated.

The aim of this work is to investigate the influence of disperse particles and the deformation temperature on the formation of ultrafine-grained structure in the Cu–Cr–Zr alloy, and to establish the influence of microstructural changes on the physical and mechanical properties of the alloy.

## EXPERIMENTAL

A Cu–0.3% Cr–0.5% Zr (wt %) alloy was selected as the material to be studied. The alloy was heated at 920°C for 0.5 hours and water cooled (quenching) to achieve a supersaturated solid solution. After quenching, the structure contained coarse Cr particles and particles enriched with zirconium, which did not dissolve at 920°C. The grain size was 120 μm. Some samples were additionally aged at 450°C for one hour and cooled in water. After aging, the structure exhibited disperse Cr particles 2–4 nm in size. To learn more about the initial microstructure, see [12]. Samples 14 × 14 × 900 mm in size after quenching or quenching followed by aging were deformed by equal channel angular pressing (ECAP) in a die with an angle of 90°C between the channels at temperatures of 473, 573, and 673 K. Four ECAP passes were carried out by

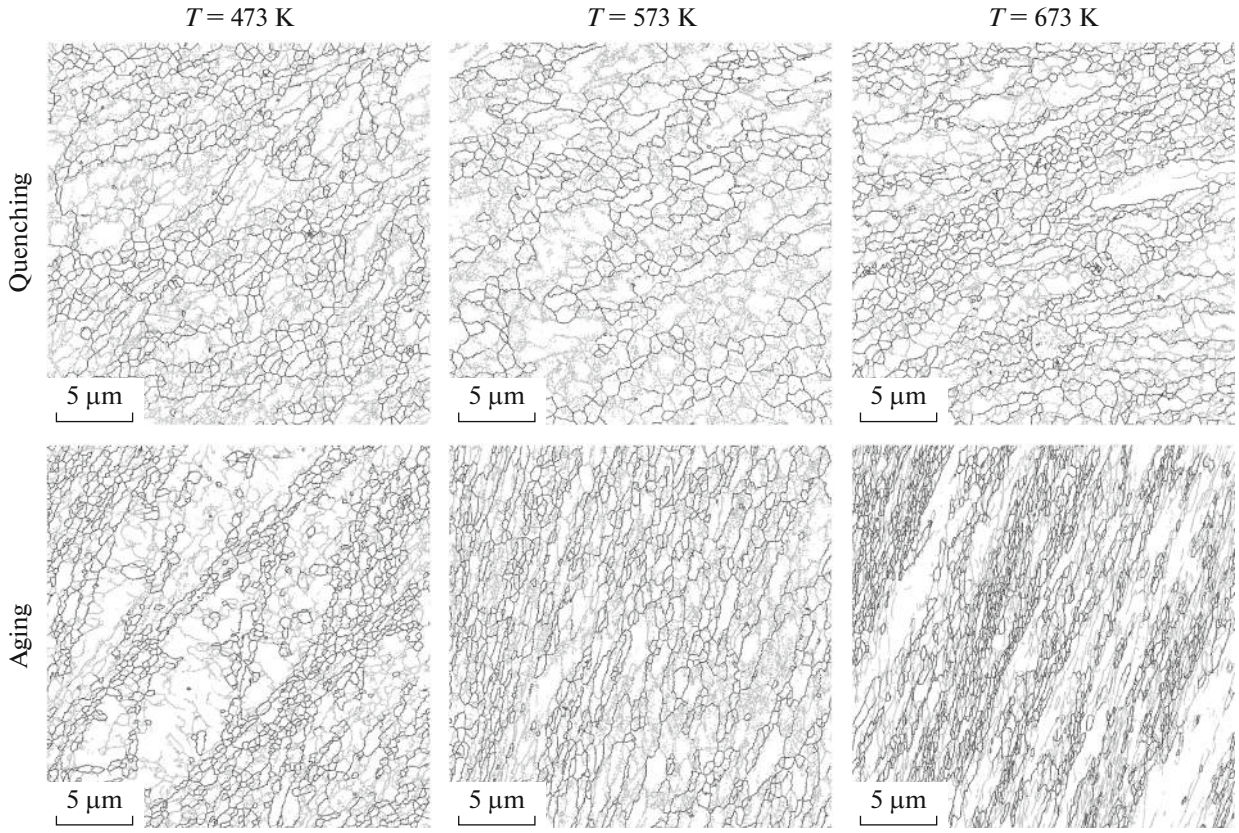


**Fig. 1.** Distribution of crystallite boundaries in the Cu–Cr–Zr alloy after quenching and aging followed by ECAP at temperatures of 473, 573, and 673 K. Gray lines indicate low-angle boundaries (<15°) and black lines indicate high-angle boundaries (>15°).

a $B_c$ route (a sample was rotated by 90° relative to the strain axis after each pass).

Tensile tests were carried out at room temperature and a tensile rate of 2 mm/min on an Instron 5882 testing machine. Flat samples with a length of the gage part of 6 mm and a cross-section of 1.5 × 3 mm, for mechanical tests, were cut out along the pressing direction. The Vickers hardness was measured using a WOLPERT 420 MVD tester at a load of 100 g and a loading time of 15 s. The number of measurements was at least 10 and the measurement error was in the range of 3–7%. In contrast to previous works, the electrical conductivity was measured by the eddy current technique using a Constant K-6 tool. The relative measurement error was 1–3%. The number of measurements was at least 10.

The microstructure was examined using a Nova NanoSem 450 FEI scanning electron microscope (SEM) equipped with a diffraction detector of backscattered electrons and a Jeol Jem 2100 transmission electron microscope (TEM) in the cross-section of samples parallel to the pressing direction. Samples were prepared by electrolytic polishing in 25% $HNO_3$ and 75% $CH_3OH$ at temperature of –20°C and a voltage of 10 V, by means of a TenuPol-5 equipment. Average grain size $D$ was determined from electron backscattered diffraction patterns by the equivalent diameters method. Fraction of high-angle boundaries (HABs) $F_{HAB}$, value of microstresses $\theta_{KAM}$ (Kernel Average Misorientation), and fraction of the UFG structure (the fraction of grains with an average size of smaller than 2 μm) $F_{UFG}$ were estimated using OIM Analysis software (scanning step of 50). TEM data were used to estimate subgrain size $d$ by the intercept method. Dislocation density ρ was determined by the number of dislocation lines visible on the foil surface. Volume fraction of particles $f_{part}$ was found using TEM images and the following ratio [13]:

$$f_{part} = \frac{2N_s}{3\pi r^2}, \quad (1)$$

where $N_s$ is the number of particles per unit area and $r$ is the average particle radius.

## RESULTS AND DISCUSSION

### *1. Microstructure of the Cu–Cr–Zr Alloy after ECAP at High Temperature*

Figure 1 shows the microstructure of the Cu–Cr–Zr alloy after ECAP at the temperatures under study. Plastic deformation results in the formation of a dense network of low-angle boundaries (LABs) of deforma-

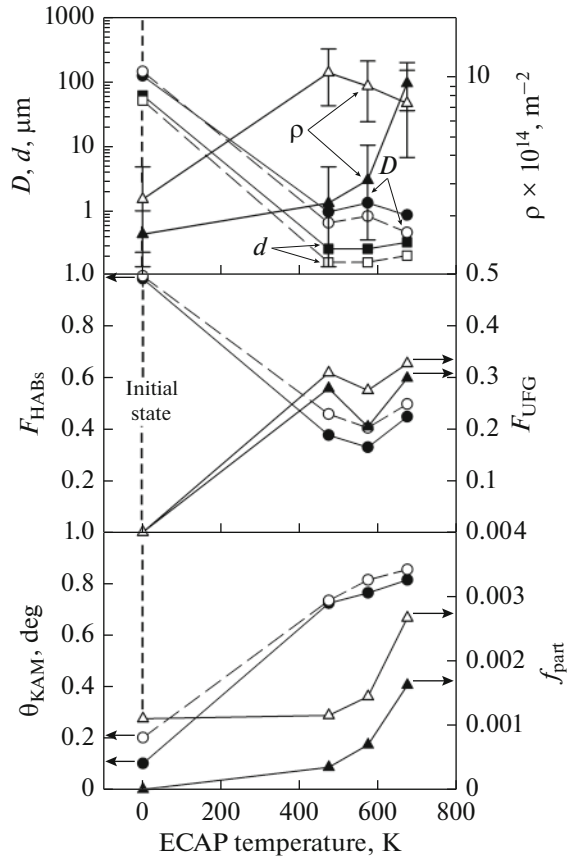


**Fig. 2.** Effect of ECAP temperature on the average size of grains ($D$) and subgrains ($d$), dislocation density ($\rho$), fraction of high-angle boundaries ($F_{HAB}$) and ultrafine-grained structure ($F_{UFG}$), internal microstresses ($\theta_{KAM}$), and volume fraction of disperse particles $f_{part}$ in the Cu–Cr–Zr alloy. Solid symbols correspond to quenching and open symbols correspond to aging.

tion origin. Crystals 0.3–0.5 μm in size, which are surrounded only by HABs, i.e., new ultrafine grains form. The UFG structure forms mainly inside deformation bands, the regions formed by long parallel HABs. This process is less pronounced in preliminary quenched samples. The thickness of deformation bands in Cu–Cr–Zr alloy after aging increases with increasing deformation temperature. The average grain size is about 1 μm (Fig. 2). The average size of structural elements in the samples after aging is lower than that after quenching. The fraction of HABs and the UFG structure is approximately 0.4 and 0.3, respectively. Preliminary aging increases these parameters by ≈0.1 regardless of the deformation temperature.

A high density of dislocations was observed in the samples after ECAP (Fig. 3). The dislocation number density in the quenched alloy increases from $2 \times 10^{14}$ to $9 \times 10^{14}$ m$^{-2}$ with increasing deformation temperature from 473 to 673 K, whereas it in the aged alloy decreases slightly from $1 \times 10^{15}$ to $7 \times 10^{14}$ m$^{-2}$ with increasing deformation temperature. Internal microstresses regardless of the initial state grow slightly within the range 0.70°–0.85° as the deformation temperature increases. Deformation at elevated temperatures causes the decomposition of the SSS and (additional) precipitation of disperse particles in the alloy, regardless of the preliminary HT. The volume fraction of the particles in the alloy after aging is 1.5–3 times higher than that in the alloy after quenching. This difference decreases as the deformation temperature increases.

### *2. Physical and Mechanical Properties of the Cu–Cr–Zr Alloy*

After quenching, the alloy has a relatively low yield strength and a large elongation. Aging increases the yield strength by 100 MPa and decreases the relative elongation by 25% (Fig. 4). Deformation at an elevated temperature increases the yield strength, the ultimate tensile strength, and decreases the relative elongation. Preliminary quenching increases the yield strength and the ultimate tensile strength of the alloys with increasing strain temperature. They are 465–490 and 475–530 MPa, respectively. The yield strength of the Cu–Cr–Zr alloy after aging does not change when the deformation temperature increases. The ultimate tensile strength after deformation at 473–573 K is 550 MPa. The highest ultimate tensile strength is 570 MPa after deformation at 673 K. The relative elongation after deformation at temperatures of 473–573 K is 7–9% irrespective of the preliminary HT. Deformation at a temperature of 673 K increases the plasticity to 20 and 22% for quenched and aged samples, respectively.

The hardness increases insignificantly with increasing deformation temperature, namely, from 161 to 169 HV for the preliminary hardened alloy and from 189 to 195 HV for the aged alloy. We should note that these values change within the hardness measurement error. The electrical conductivity of the initial alloy after quenching is 35% IACS (percentage of electrical conductivity of pure annealed copper), and after aging, 47% IACS. ECAP at a high temperature results in increased conductive properties of the Cu–Cr–Zr alloy, no matter what the HT is. A further increase in the deformation temperature causes the conductive properties to grow. The maximum conductivities of Cu–Cr–Zr alloy are 51 and 65% IACS after quenching and deformation and after aging and deformation, respectively.

### *3. Effect of Deformation Aging on the Structure and Properties of the Cu–Cr–Zr Alloy*

An increase in the electrical conductivity of the Cu–Cr–Zr alloy indicates the decomposition of the SSS during deformation and the precipitation of disperse particles, i.e., deformation aging, which is

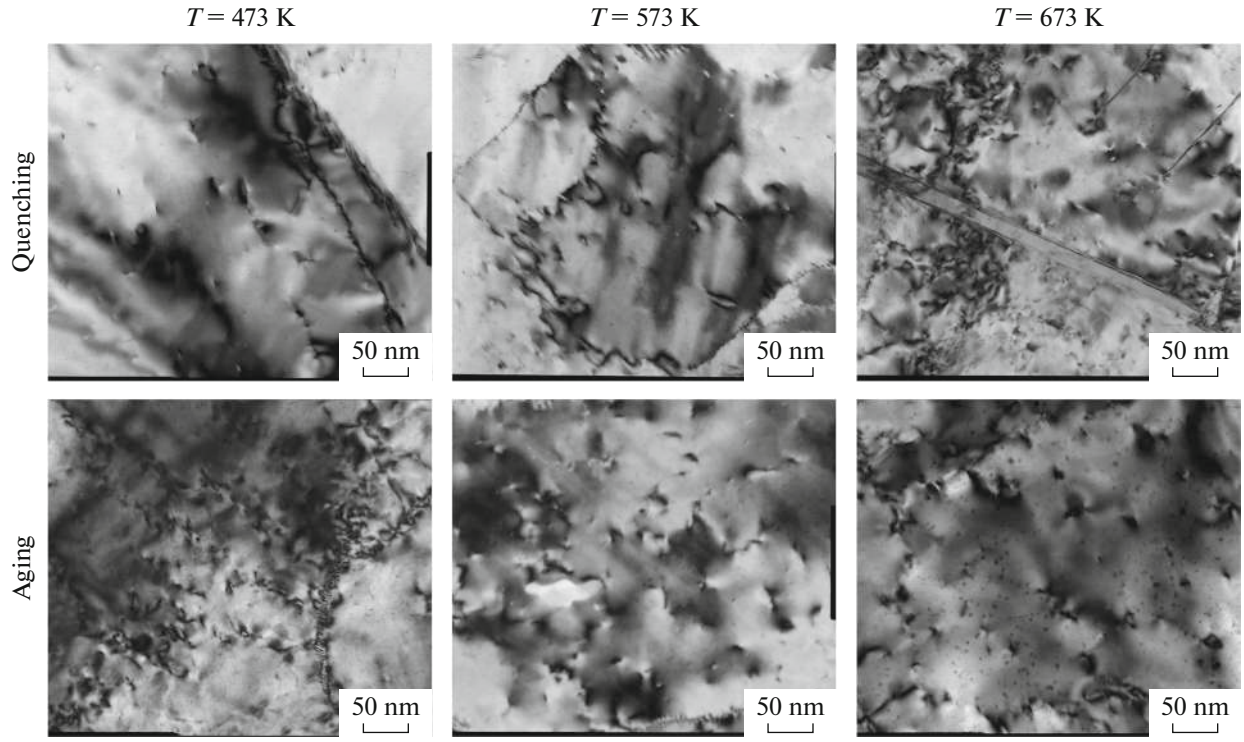


**Fig. 3.** Microstructure of the Cu–Cr–Zr alloy after quenching and aging followed by ECAP at temperatures of 473, 573, and 673 K.

confirmed by TEM data. Fraction of SSS decomposition $f_{dec}$ can be expressed using electrical resistivity Ω (the value that is opposite to the electrical conductivity) in the following way [14]:

$$f_{dec} = \frac{\Omega - \Omega_0}{\Omega_{max} - \Omega_0}, \quad (2)$$

where $\Omega_{max}$ and $\Omega_0$ are electrical resistivity before and after the phase transformation, respectively. The electrical resistivity is maximum $\Omega_{max}$ after quenching. Its value is $4.92 \times 10^{-8}$ Ω m. Electrical resistivity $\Omega_0$ was measured after annealing at 550°C for 24 hours and was $2.15 \times 10^{-8}$ Ω m. Figure 5 shows a fraction of the SSS decomposed as a function of the deformation temperature. The decomposition rate of the SSS in the preliminary quenched alloy is higher than that in the aged alloy. The rate of the SSS decomposition is a function of the preliminary HT due to a decrease in the driving force of the phase transformation $\Delta g$, because of the decrease in the content of alloying elements in the solid solution according to the Russell approach [15]:

$$\Delta g = -\frac{kT}{\nu_{at}} \ln\left(\frac{C}{C_{eq}}\right), \quad (3)$$

where $k$ is the Boltzmann's constant, $T$ is the temperature, $\nu_{at}$ is the atomic volume, $C$ is the concentration of alloying elements in the solid solution, and $C_{eq}$ is the equilibrium concentration of alloying element in the solid solution.

If the concentrations of Cr and Zr in the matrix after quenching are 0.003 and 0.002 (the last corresponds to the solubility limit of Zr in the copper matrix [9]), respectively, and those of Cr and Zr after aging are 0. 00093 and 0.00062 (according to calculation of the fraction of SSS decomposed), the driving force of the precipitation of disperse particles according to Eq. (3) is 1.7 times greater than that in the preliminary quenched alloy.

Note that the volume fraction of the precipitated particles observed by TEM is in good agreement with the fraction of SSS decomposed (approximation confidence ratio $R^2 = 0.96$). Deformation tends to localize within deformation bands (Fig. 1), the dislocation density and microstress level tend to grow, and the average grain size tends to decrease (Fig. 5) in the Cu–Cr–Zr alloy with increasing fraction of the decomposed SSS. Precipitation of disperse particles from SSS during deformation can retard dynamic recovery and increase the dislocation density, and, therefore, increase microstresses in the alloy. Particles, as additional obstacles, can pin dislocations and reduce their mobility, thus, favoring the bending of dislocations and the formation of new dislocation loops. An increase in the dislocation density and the corresponding growth of microstresses lead to the microstructural fragmentation, i.e., the formation of deformation-induced grain boundaries. However, dynamic recovery processes are activated, as the deformation temperature increases. These processes,

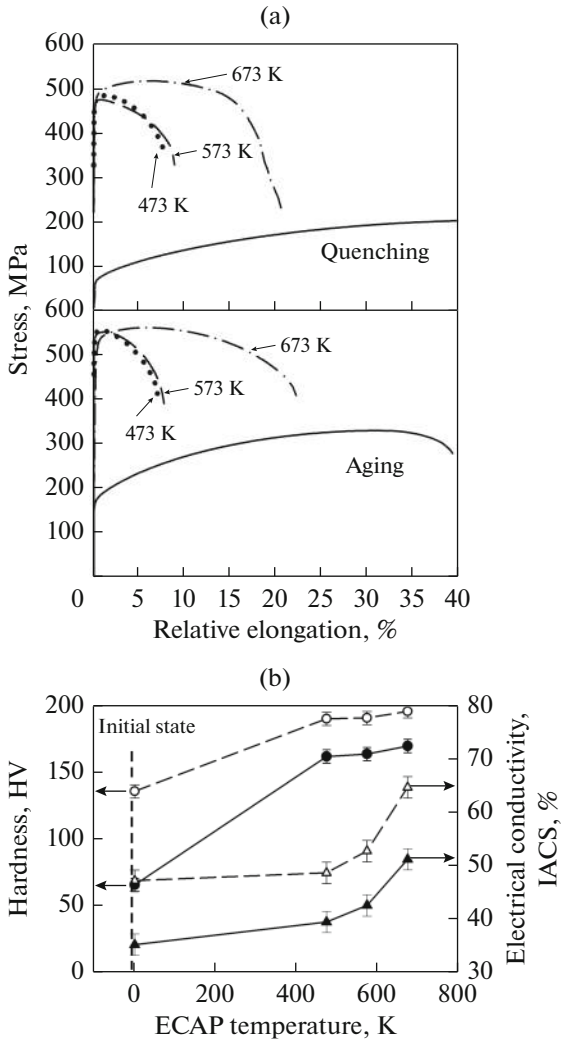


**Fig. 4.** (a) Stress-strain curve of the Cu–Cr–Zr alloy after quenching and aging followed by ECAP at 473, 573, and 673 K. (b) Effect of the ECAP temperature on (●, ○) hardness and (△, ▲) electrical resistivity of the Cu–Cr–Zr alloy. Solid symbols correspond to quenching and open symbols correspond to aging.

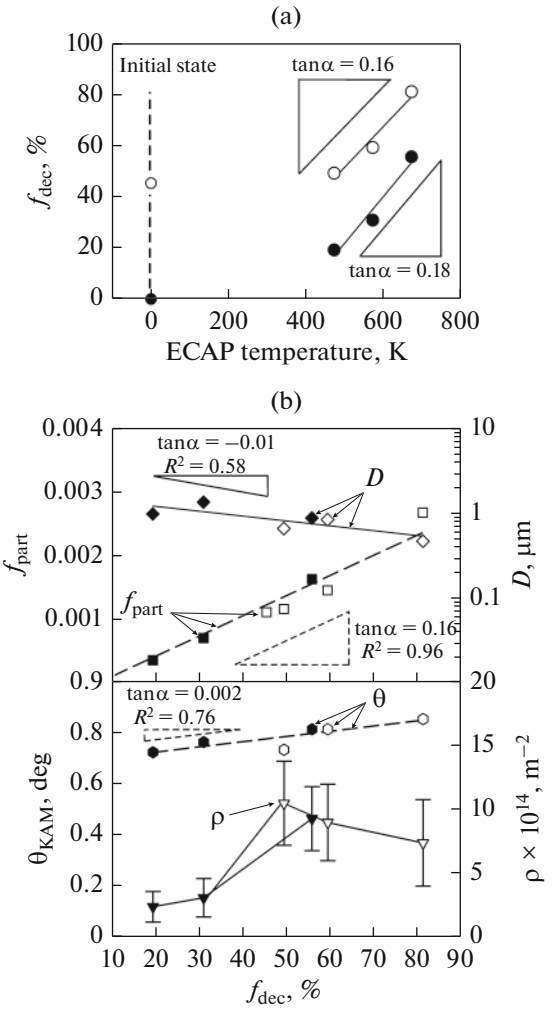


**Fig. 5.**(a) Temperature effect on the decomposition of the supersaturated solid solution. (b) The volume fraction of disperse particles ($f_{part}$), grain size ($D$), microstresses ($\theta_{KAM}$), and dislocation density (ρ) as functions of supersaturated solid solution decomposition. Solid symbols correspond to quenching and open symbols correspond to aging.

on the one hand, reduce the density of dislocations and, on the other hand, facilitate continuous dynamic recrystallization. Precipitation hardening and dynamic recovery, as two competing processes, control the dynamic recrystallization rate, grain size, and dislocation density, resulting in a different behavior of the dislocation density as a deformation temperature in the preliminary quenched and aged alloy. The grain size and dislocation density influence the strength properties of the alloy in accordance with the well-known Hall–Petch and Taylor relations, respectively [8]. The precipitation of disperse particles during deformation ensures high strength properties of the copper alloys due to both precipitation hardening and dislocation and grain boundary hardening.

Deformation-induced aging increases the number of structural defects, such as particles, dislocations, grain boundaries, by which electrons can be scattered during their motion under the application of the potential difference. However, the electrical conductivity during the experiment increases with increasing SSS decomposition fraction, dislocation density, and grain boundaries (inverse to the grain size value). These experimental data can be explained by a different degree of influence of dislocations, crystallite boundaries, and substitution atoms on the conductivity of metallic materials. It is substitution atoms that have a major effect on the conductive properties of copper alloys [1, 9]. A rise in conductivity due to a decreasing concentration of alloying elements in solid solution to a great extent exceeds a decrease in con-

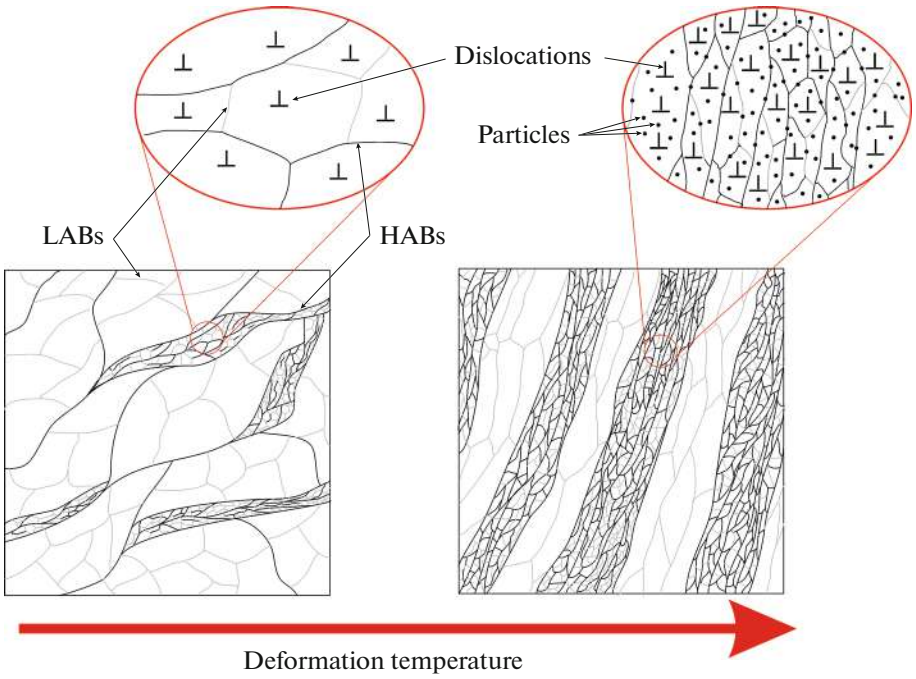


**Fig. 6.** Schematic representation of structural evolution in the Cu–Cr–Zr alloy during ECAP at various temperatures.

ductive properties due to electrons scattering by other structural defects. Therefore, precipitation of disperse particles before or during deformation is crucial for the formation of the optimal structure that ensures the high strength and electrical conductivity of the Cu–Cr–Zr alloys.

These results have been used to develop a graphical model of deformation temperature influence on the Cu–Cr–Zr alloy structure, which is illustrated in Fig. 6. An increase in the deformation temperature causes the decomposition of the supersaturated solid solution and the precipitation of disperse particles. These particles enable the localization of deformation in the bands and facilitate the accumulation of a high dislocation density, resulting in the formation of a structure with smaller crystallite sizes, larger fractions of HABs and the UFG structure.

## CONCLUSIONS

ECAP of the Cu–0.3% Cr–0.5% Zr alloy at an elevated temperature forms a dense network of LABs of deformation origin and a UFG structure in some regions, which enhances the strength properties significantly.

Deformation at elevated temperatures leads to the decomposition of the SSS and the precipitation of disperse particles. The fraction of the SSS decomposed increases with increasing deformation temperature.

The deformation-induced precipitation of disperse particles results in the formation of localized deformation bands, decrease in the grain size, increase in the dislocation density, and the fraction of HABs and UFG structure.

Preliminary aging of the alloy increases the efficiency of the ECAP with respect to the improvement of strength and electrical conductivity. The strength of the alloy after aging and ECAP at 673 K is 570 MPa and its electrical conductivity is 65% IACS.

## ACKNOWLEDGMENTS

The authors are grateful to the personnel of the Joint Research Center, “Technology and Materials,” Belgorod National Research University, for their assistance with instrumental analysis.

## FUNDING

The financial supports received from the Ministry of Science and Higher Education of the Russian Federation, under President grant no. 075-15-2020-407 for microstructure investigation, and from the Russian Science Foundation, Russia, under grant no. 19-79-30025 for mechanical property analysis, and financial support of the Ministry of Science and Higher Education of Russian Federation in the frame work of Increase Competitiveness Program of NUST “MISIS” are gratefully acknowledged.

## REFERENCES

1. M. Y. Murashkin, I. Sabirov, X. Sauvage, and R. Z. Valiev, “Nanostructured Al and Cu alloys with superior

strength and electrical conductivity," J. Mater. Sci. **51** (1), 33–49 (2016).

2. V. I. Zel'dovich, S. V. Dobatkin, N. Yu. Frolova, I. V. Khomskaya, A. E. Kheifets, E. V. Shorokhov, and P. A. Nasonov, "Mechanical properties and the structure of chromium–zirconium bronze after dynamic channel-angular pressing and subsequent aging," Phys. Met. Metalogr. **117**, 74–82 (2016).
3. N. Liang, J. Liu, S. Lin, Y. Wang, J. T. Wang, Y. Zhao, and Y. Zhu, "A multiscale architectured CuCrZr alloy with high strength, electrical conductivity and thermal stability," J. Alloys Compd. **735**, 1389–1394 (2018).
4. A. Vinogradov, Y. Suzuki, T. Ishida, K. Kitagawa, and V. I. Kopylov, "Effect of chemical composition on structure and properties of ultrafine grained Cu–Cr–Zr alloys produced by equal-channel angular pressing," Mater. Trans. **45** (7), 2187–2191 (2004).
5. N. V. Melekhin and V. N. Chuvil'deev, "Influence of equal-channel-angular pressing on the particle precipitation in the Cu–Cr–Zr alloy," Vestn. Nizhegorodsk. Univ. im. N.I. Lobachevskogo, No. 5, 55–61 (2011).
6. A. Chbihi, X. Sauvage, and D. Blavette, "Atomic scale investigation of Cr precipitation in copper," Acta Mater. **60** (11), 4575–4585 (2012).
7. H. Fuxiang, M. Jusheng, N. Honglong, G. Zhiting, L. Chao, G. Shumei, Y. Xuetao, W. Tao, L. Hong, and L. Huafen, "Analysis of phases in a Cu–Cr–Zr alloy," Scr. Mater. **48** (1), 97–102 (2003).
8. D. V. Shangina, V. F. Terent'ev, D. V. Prosvirnin, O. V. Antonova, N. R. Bochvar, M. V. Gorshenkov, G. I. Raab, and S. V. Dobatkin, "Mechanical properties, fatigue life, and electrical conductivity of Cu–Cr–Hf alloy after equal channel angular pressing," Adv. Eng. Mater. **20** (1), 1700536 (2018).
9. A. Morozova, R. Mishnev, A. Belyakov, and R. Kaibyshev, "Microstructure and properties of fine grained Cu–Cr–Zr alloys after termo-mechanical treatments," Rev. Adv. Mater. Sci. **54** (1), 56–92 (2018).
10. R. K. Islamgaliev, K. M. Nesterov, and R. Z. Valiev, "Structure, strength, and electric conductivity of a Cu–Cr copper-based alloy subjected to severe plastic deformation," Phys. Met. Metallogr. **116**, 209–218 (2015).
11. M. Murayama, A. Belyakov, T. Hara, Y. Sakai, K. Tsuzaki, M. Okubo, M. Eto, and T. Kimura, "Development of a high-strength high-conductivity Cu–Ni–P alloy. Part I: Characterization of precipitation products," J. Electron. Mater. **35** (10), 1787–1792 (2006).
12. A. P. Zhilyaev, I. Shakhova, A. Morozova, A. Belyakov, and R. Kaibyshev, "Grain refinement kinetics and strengthening mechanisms in Cu–0.3Cr–0.5Zr alloy subjected to intense plastic deformation," Mater. Sci. Eng. A **654**, 131–142 (2016).
13. F. J. Humphreys and M. Hatherly, *Recrystallization and Related Annealing Phenomena* (Elsevier, Amsterdam, 2012).
14. Y. Zhang, A. A. Volinsky, H. T. Tran, Z. Chai, P. Liu, B. Tian, and Y. Liu, "Aging behavior and precipitates analysis of the Cu–Cr–Zr–Ce alloy," Mater. Sci. Eng., A **650**, 248–253 (2016).
15. H. I. Aaronson, K. R. Kinsman, and K. C. Russell, "The volume free energy change associated with precipitate nucleation," Scr. Metall. **4** (2), 101–106 (1970).

*Translated by T. Gapontseva*